Original Article

Atlantoaxial Langerhans cell histiocytosis radiographic characteristics and corresponding prognosis analysis

ABSTRACT

Background: Langerhans cell histiocytosis (LCH) may affect atlas and axis, and there were very few published cases describing a characteristic of LCH of atlantoaxial.

Objective: The objective of the study is to investigate the image manifestations of atlantoaxial LCH to improve the in-depth comprehension on it.

Materials and Methods: A retrospective study was done of computed tomography (CT) and magnetic resonance imaging in atlas and axis and prognosis was analyzed.

Results: The study included 41 patients (average age 12.9 years and median age 8 years) diagnosed with LCH, with 75.6% under 15 years old. Eighty-four lesions of LCH were identified including 47 in the atlas and 37 in the axis. The osteolytic bone destructions in the atlas and axis were characterized, 22% accompanied by sclerotic margins. Thirteen patients had a compression fracture, 11 in the lateral mass of the atlas and 2 in the C2 vertebral body. Sixteen and three patients had atlantoaxial malalignment and dislocation, respectively. On T2-weighted images, 68.9% showed iso- or low-signal intensity, 27.6% showed hyperintensity signal, and 3.4% showed heterogeneous signal. On postcontrast images, 81.9% showed significant enhancement, 12.5% showed moderate enhancement, and 6.3% showed mild enhancement. CT reexamination of 14 patients indicated atlantoaxial bone destruction relatively repaired in 12 patients. Thirty-three patients were a follow-up, 81.8% had no significant symptoms and 18.2% with remaining symptoms.

Conclusions: The atlas and axis were affected by LCH, mainly in children. The lateral mass was easily affected and compressed, destruction of the atlas and axis could lead to atlantoaxial joint instability. The prognosis was good in most of the patients.

Keywords: Atlantoaxial, Langerhans cell histiocytosis, spine

INTRODUCTION

Langerhans cell histiocytosis (LCH) is a heterogeneous illness characterized by the proliferation of dendritic cells. LCH refers to a spectrum of diseases, clinical variants of LCH include eosinophilic granuloma the most benign variant that either single or multifocal bone lesion without visceral involvement, Hand–Schu¨ller–Christian disease and Letterer–Siwe disease.[1] Now, the new trend is divided into three groups on the basis of the number of LCH lesions and systems involved and include unifocal form, multifocal unisystem, and multifocal multisystem.[2] It was reported that 80% of patients with LCH had their skeleton system affected and 6.5%–25% had the spine affected. The thoracic vertebrae were the most commonly affected (54%), followed by lumbar (35%), and cervical vertebrae (11%).[3] However, satisfactory reports on the incidence of LCH of the atlas and axis are lacking.

The atlas and axis belong to high cervical spine with special anatomic structure. Atlantoaxial LCH can result in dislocation

Lihua Zhang, Liang Jiang[1], Huishu Yuan, Zhongjun Liu[1], Xiaoguang Liu[1]

Departments of Radiology and [1]Orthopaedics, Peking University Third Hospital, Beijing, PR China

Address for correspondence: Prof. Huishu Yuan,
Department of Radiology, Peking University Third Hospital, Beijing, PR China. E-mail: huishuyuan69@126.com
Prof. Zhongjun Liu, Department of Orthopaedics, Peking University Third Hospital, Beijing, PR China.
E-mail: liuzj@medmail.com.cn

How to cite this article: Zhang L, Jiang L, Yuan H, Liu Z, Liu X. Atlantoaxial Langerhans cell histiocytosis radiographic characteristics and corresponding prognosis analysis. J Craniovert Jun Spine 2017;8:199-204.

and spine cord suppression. Therefore, an early and accurate diagnosis of atlantoaxial LCH is of important clinical significance. In the current study, a retrospective analysis was conducted based on the medical information of 41 patients with LCH to improve the in-depth comprehension on LCH.

MATERIALS AND METHODS

Clinical manifestation and radiographic information of 41 patients with clinical or pathological confirmed atlantoaxial LCH were collected retrospectively between January 1997 and November 2015. The image findings of computed tomography (CT) and magnetic resonance imaging (MRI) of 41 patients with LCH were analyzed by two radiologists to evaluate the lesion number, location, bone destruction type, integrity of bone cortex, sclerotic margin, paraspinal soft tissue masses, atlantoaxial dislocation, MRI signal intensity, and enhancement feature. The patients were followed up for 4 months to 5 years.

RESULTS

Demographics data

The study group comprised 25 men and 16 women, a male-female ratio of 25:16. The mean age was 12.9 years for the group, and median age was 8 years old. Child under 15-year-old and adults accounted for 75.6% and 24.4%, respectively. The main clinical symptom was the neck pain; 23 and 8 patients also had movement limitation and neck deflection, respectively.

Location and numbers of Langerhans cell histiocytosis

Of the 41 LCH cases, 22 cases were located in the atlas, 17 located in the axis, and 2 involved C1–C2. The total number of LCH lesions was 84 including 47 in atlas and 37 in axis. Among 47 lesions in atlas, there were 12 lesions (14%) located in anterior arch, 14 lesions (16%) located in posterior arch, and 21 lesions (25%) located in lateral mass. Among 37 lesions in axis, there were 8 lesions (10%) located in odontoid process, 17 (20%) located in veterbral body, and 12 (14%) located in attachment. Anterior arch, posterior arch, and lateral mass were all involved in 12 atlas, veterbral body and attachment were involved in 11 axis, accounting for 55% and 29%, respectively.

Computed tomography imaging findings

The type of bone destruction was diversified, including geographic (15, 37%), moth-eaten (7, 17%) bone destructions with clear margin, and penetrating (19, 46%) bone destructions without clear margin. The bone cortex was destroyed and the integrity was compromised in 29 (71%) patients [Figure 1a and b]. The sclerotic margins around the bone destruction were found in 9 (22%) patients [Figures 3a,b and 4a-c]. In addition, the compression fracture

was found in 13 patients, including 11 in the lateral mass of the atlas, and 2 in C2 vertebral body [Table 1].

Atlantoaxial malalignment

Sixteen (39%) patients had atlantoaxial malalignment, manifested as an unequal distance between the odontoid and the bilateral mass [Figure 2a and b]. Three (7%) patients had anterior dislocations.

Magnetic resonance imaging signal

T1-weighted MR images showed homogeneous and similar signal intensity to the normal spinal cord in 20 patients (68.9%) [Figures 2c, 3c and 4d], low signal intensity in 7 patients (24.1%), and high signal intensity in 2 patients (6.9%). T2-weighted MR images showed iso-intensity in 17 patients (58.6%) [Figures 2d, 3d and 4e], low signal intensity in 3 (10.3%), high signal intensity in 8 (27.6%), and heterogeneous signal in 1 (3.4%). Multiple fluid–fluid levels were seen in two cases; after gadolinium administration, 13 (81.3%) tumors showed significant enhancement [Figures 1d, 1e, 2e, 2f and 3e], two (12.5%) showed moderate enhancement [Figure 4f], and one (6.3%) showed mild enhancement [Table 2].

Paravertebral, intraspinal mass, and paravertebral soft swelling

Paravertebral soft tissue mass was seen in 26 cases [Figures 1c and 2f], accounting for 26%; intraspinal mass was seen in 2 cases,

Table 1: CT character of LCH in atals-axis

CT Character	Number	Proportion
Location		
Atlas	22	54%
Axis	17	41%
Atlas-axis	2	5%
Imcomplete cortex	29	71%
Sclerosis rim	9	22%
Pathological fracture	13	31.7%

Table 2: MRI character of LCH in atals-axis

MRI Character	Number	Proportion
T1WI		
Iso-intensity signal	20	68.9%
Low signal	7	24.1%
High signal	2	6.9%
T2WI		
Iso-intensity signal	17	58.6%
Low signal	3	10.3%
High signal	8	27.6%
Heterogenous signal	1	3.4%
Post-contrast		
Mild enhancement	1	6.3%
Moderate enhancement	2	12.5%
Significant enhancement	13	81.3%

accounting for 4.8%. Twenty-six cases were accompanied with paravertebral soft tissue swelling, accounting for 66%.

Computed tomography reexamination results of 14 patients

The patients were followed up for 4–60 months. The height of the atlas lateral mass was restored in six patients, and one patient had significant sclerotic margin. Two patients had significant sclerosis in the C2 vertebral body, three patients had a decreased bone destruction area of C2 [Figure 2g and h], one patient had no obvious improvement, and another patient had an increased number of lesions [Table 3].
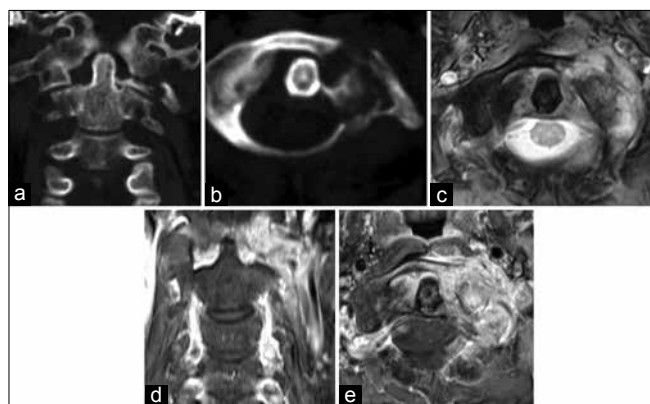

Figure 1: Langerhans cell histiocytosis of C1 lateral mass in a 45-year-old man with neck pain. Cornal (a) reformatted computed tomography images scan revealed that the left lateral mass of C1 was depressed. Axial (b) showed the lytic bone destruction of the left lateral mass and the bone cortex was not complete. Axial (c) T2-weighted fast spin-echo magnetic resonance images showed the bone destruction of C1 lateral mass with soft mass formation. On cornal (d) and axial (e) gadolinium-enhanced T1-weighted image showed the significant enhancement of C1 lateral mass and adjacent soft mass

Clinical and follow-up

Thirty-eight clinical treatment data were collected and 24 patients received conservative treatment including 9 observations and 15 scaffold used, 3 patients received surgery, 7 received radiation, and 4 received chemotherapy.

Thirty-three patients were followed up from 18.2 to 151 months and mean was 66 months. It was found that 27 (81.8%) patients had no symptoms and 6 (18.2%) patients with associated symptoms.

DISCUSSION

LCH represents a disorder characterized by the abnormal of Langerhans cell proliferation and can be associated with inflammatory cells and multinucleated giant cell infiltration. It can affect any organ, tissue and it is associated with the immune-mediated process.[4] LCH may manifest at any age, and the peak age is from 1 to 3 years[5] or 5–10 years.[6] The mean age of this group was 12.9-year-old, the median age was 8-year-old and patients under 15 years accounting for 75.6%. It was estimated that 75%–80% of LCH manifested as bone destruction,[7] especially in flat bone and spine. It was common seen in thoracic spine and more than half of the cervical LCH lesions affected the C3–C5 vertebrae,[8] and there were very few published cases describing LCH of atlas and axis. This study showed that it was not rare LCH in atlas and axis. The main manifestation of LCH in the atlas and axis was the neck pain. Limited movement as an accompanying symptom could be found in some patients. The main reasons
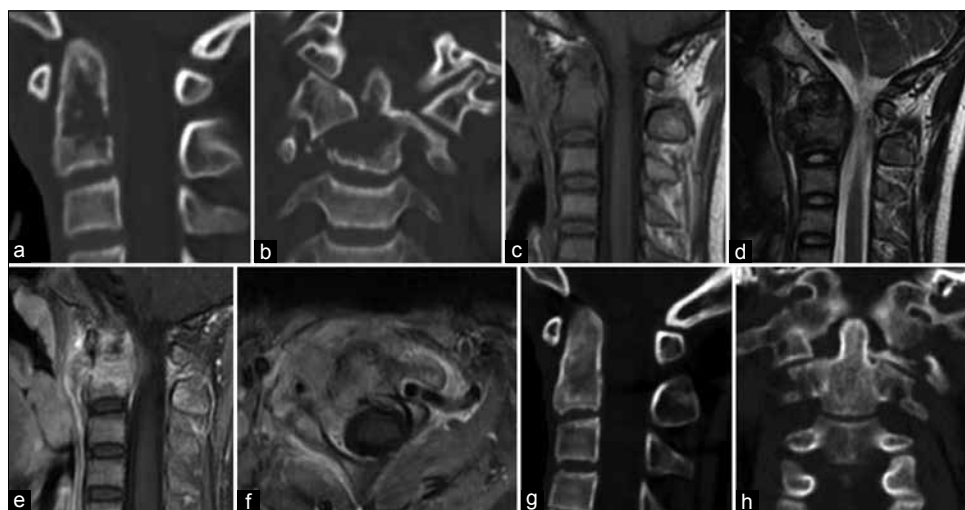

Figure 2: LCH of C2 in a 14-year old child. Sagittal (a) reformatted computed tomography images scan revealed that vertebrae of C2 bone destruction with penetrating into the posterior margin. Cornal (b) reformatted computed tomography images scan showed that the destruction of C2 and dislocation of C1–C2. (c) Sagittal T1-weighted images showed that C2 lesion was isointensity. T2-weighted (d) images showed that C2 lesion was isointensity. On sagittal (e) gadolinium-enhanced T1-weighted image showed the significant enhancement. Axial (f) showed the dural sac was compressed with narrowing of spinal canal. Computed tomography re-examination carried out 2 years later showed that bone destruction of C2 was repaired on sagittal (g). Cornal (h) images showed repairment in C2

Table 3: Follow-up CT reexamination results of 14 patients

| Case (NO)	Location	Age (years)	CT features (examination)	Follow-up time (months)	CT features (reexamination)
1	Lateral mass	1	Bone destruction with flatten	12	Height restored
2	Lateral mass	3	Bone destruction with flatten	12	Height restored
3	Lateral mass	5	Bone destruction with flatten	48	Height restored
4	Lateral mass and anterior arch	9	compressed	12	Height restored
5	Lateral mass and anterior arch	10	compressed	12	Height restored
6	Lateral mass	10	compressed	3	Bone sclerosis
7	Lateral mass	14	compressed	12	Height restored
8	Vertebral body and attachment of C2	4	Bone destruction	4	Bone sclerosis
9	Vertebral body and attachment of C2	14	bone destruction	24	Bone destruction Decreased
10	Vertebral body of C2	25	Bone destruction	12	Bone destruction Decreased
11	Vertebral body and attachment of C2	52	Bone destruction	24	Bone destruction Decreased
12	C1-2	8	Bone destruction	60	Sclerosis
13	Vertebral body and attachment of C2	5	Bone destruction with cortical penetrating	11	stable
14	C1-2	2	Bone destruction	2	progress
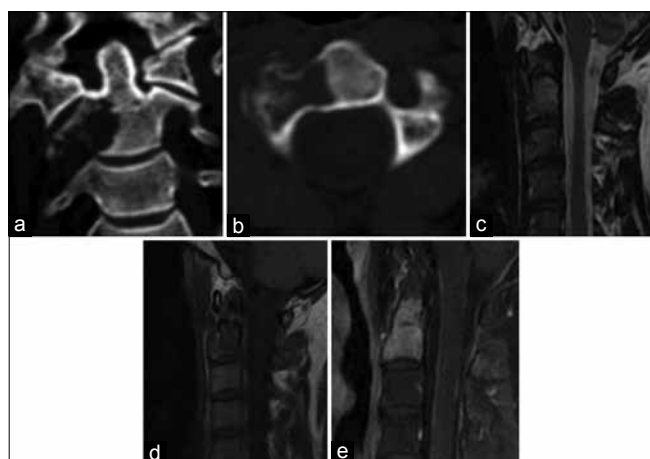
Figure 3: LCH of C2 in a 26-year old man. Cornal (a) reformatted computed tomography image scan revealed that vertebrae of C2 bone destruction, with C2 right rim bone cortex incomplete and sclerosis rim formation in the left of C2. Axial (b) reformatted image showed that right transverse foramen of C2 was involved. Sagittal T2-weighted (c) showed that C2 lesion was isointensity. Sagittal T1-weighted (d) images showed that C2 lesion was isointensity. On sagittal (e) gadolinium-enhanced T1-weighted image showed the significant enhancement of C2 lesion
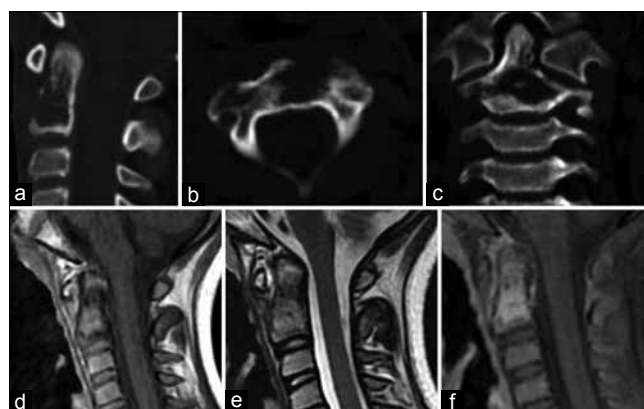

Figure 4: LCH of C2 in 9-year old female. Sagittal (a) reformatted computed tomography images scan revealed that lytic cone destruction in vertebrae of C2 with clear margin. Axial (b) reformatted computed tomography images scan revealed bone sclerosis around bone destruction. Cornal (c) reformatted images showed that anterior bone cortex was incomplete and bone sclerosis was seen around the bone destruction. Sagittal T1-weighted (d) images showed that C2 lesion was isointensity. Sagittal T2-weighted (e) images showed that C2 lesion was isointensity. On sagittal (f) gadolinium-enhanced T1-weighted image showed the moderate enhancement of C2 lesion

of the idiopathic neck pain and limited neck movement in children were LCH and osteomyelitis, and it should be considered for differential diagnosis.[9]

The atlas and axis are located to the high level of cervical spine and at the junction of the skull and neck with special anatomic structure. CT is an important radiographic tool for LCH diagnosis and highly advantageous in displaying the types of bone destruction and atlantoaxial alignment. The atlas is composed of three parts including the anterior and posterior arches and the lateral mass. The bone destruction occurred nearly equally in the anterior (14%) and posterior arches (16%). The lateral mass is connected to the anterior and posterior arches. Its top and bottom surfaces form

joints with the occipital condyle and the superior articular surface of the axis, respectively. The lateral mass was easily affected by LCH (25% in the present study). The bone destruction of the lateral mass could lead to the movement restriction of the atlantooccipital joint and atlantoaxial joint and was manifested as neck movement limitation. The present findings indicated that the incidence of lateral mass involvement was not only high but also severe. The lateral masses were significantly flattened with shrunk volume in 11 patients, which was considered to be related with its weight-bearing role in the spine. The severe distorted lateral mass could lead to the instability of the lateral atlantoaxial joints, which was confirmed by the present finding that 39% patients had instability of the lateral atlantoaxial joints and 7% patients had anterior dislocation. The bone destruction

of LCH was broad, and 55% patients had LCH affected in both the anterior and posterior arches and the lateral mass. The vertebral body was the main affected part in the axis the same as the lower cervical vertebrae, and the appendix of vertebrae was also easily affected. Furthermore, the present study showed that 65% of the patients had both the vertebral body and the appendix affected, which was different from a previous report that the appendix was more easily affected by LCH.[10]

The location, severity, and pathological bone fracture could be evaluated and displayed by CT,[11] which was helpful in clinical decision-making. The osteolytic destruction was the main radiographic manifestation of LCH. The margins of bone destructions were relatively clear, whereas the margins of penetrating destructions were unclear. The incomplete bone cortex was as high as 71% in the present study, representing the invasive feature of LCH.[12] The sclerotic margins and sclerosis were the characteristic features of LCH, indicating repair responses; 22% of patients had sclerotic margins. The thickness of the vertebral body could be gradually recovered along with the improvement of LCH. In the present study, 14 patients had been followed up with CT and it showed that the thickness of the atlas lateral mass was recovered in six patients, one patient had significant sclerotic margin, two patients had significant sclerosis in the C2 vertebral body, and three patients had decreased bone destruction area of C2, indicating that LCH was self-limiting. However, some patients had progressed LCH during the follow-up period, one patient had solitary lesions turned into multiple lesions, and another patient had no obvious improvement. Therefore, the regular follow-up review was necessary for patients with LCH.

LCH can extend into paraspinal and epidural space, which could be clearly revealed by MRI. The paraspinal soft tissue masses were found in 63% patients with LCH in the present study, and 4.8% patients had spinal canal soft tissue masses accompanied by spinal suppression. Once the spinal suppression was confirmed, the surgical interference was needed.[13] The paraspinal soft tissue masses were more common than the spinal canal soft tissue masses probably because the anterior mass of the vertebral body was more easily affected by LCH. Moreover, 66% of the patients had paraspinal soft tissue swelling because of inflammatory cells and eosinophilic infiltration, which was similar to infectious diseases.[14] The swelling could gradually shrink and disappear with disease improvement. The characteristic MRI signal of the paraspinal soft tissue masses was suggestive of the diagnosis of LCH. In general, the LCH signal was relatively uniform, although the T2-weighted image signals were diversified: 68.9% and 27.6% presented as

isointensity and hypointensity, respectively. It was reported that the hyperintensity signal was relatively common for LCH. However, the hypointensity signal was the major type in the present study, which might be ascribed to the different courses of LCH. The intensity was relatively higher in the acute phase and gradually decreased in the healing phase.[15,16] LCH had a relatively abundant blood supply. The significant and uniform enhanced intensity was often observed under the enhancement scanning; 81.3% patients had a significant enhanced intensity.

The LCH of children should be differentiated from osteomyelitis and Ewing's sarcoma. All of them are manifested as infiltrative and penetrating bone destruction accompanied by periosteum reaction. The paraspinal soft tissue masses of Ewing's sarcoma usually are accompanied by cystic necrosis, which is distinctive from LCH.[17] The soft tissue masses of LCH could gradually shrink with the improvement of LCH.[11] Moth-eaten bone destruction of LCH was also similar to bone tuberculosis; however, the sequestrum that was common in bone tuberculosis was very rare in LCH. In addition, the cold abscess of paraspinal tuberculosis was demonstrated as ring-like enhanced intensity under enhancement scanning, which was different from LCH.[18]

The therapeutic strategy depends on the number and location of LCH lesions. The conservative treatment is usually adopted for atlantoaxial LCH. The close medical surveillance is needed for stable lesions, whereas the scaffold is required for unstable lesions. The nerve damage symptoms and abnormalities were found in three patients, and the surgeries were performed correspondingly. Four of five patients with multiple sites of bone destruction underwent chemotherapy. Thirty-three patients were followed up, and 81.8% patients had no obvious symptoms during the follow-up period.

In summary, the atlantoaxial LCH was commonly found in children, and the bone destruction often occurred in the lateral masses of vertebrae. The bone destruction could be extended to the anterior and posterior arch of the atlas, while the vertebral body of the axis was mainly affected with the appendix involved as well. The bone destruction of the atlas and axis could lead to instability and dislocation of the atlantoaxial joint. The radiographic morphology of bone destruction was diversified with the incomplete bone cortex accompanied by paraspinal soft tissue masses or swelling. LCH was characterized as an MRI signal of isointensity and hypointensity. A significant and uniform intensity was commonly observed under enhancement scanning. The conservative treatment was usually adopted for atlantoaxial LCH, and the prognosis was generally satisfactory.

Financial support and sponsorship

Nil.

Conflicts of interest

There are no conflicts of interest.

REFERENCES

1. Hoover KB, Rosenthal DI, Mankin H. Langerhans cell histiocytosis. Skeletal Radiol 2007;36:95-104.
2. Zaveri J, La Q, Yarmish G, Neuman J. More than just Langerhans cell histiocytosis: A radiologic review of histiocytic disorders. Radiographics 2014;34:2008-24.
3. Bertram C, Madert J, Eggers C. Eosinophilic granuloma of the cervical spine. Spine (Phila Pa 1976) 2002;27:1408-13.
4. Nezelof C, Basset F. Langerhans cell histiocytosis research. Past, present, and future. Hematol Oncol Clin North Am 1998;12:385-406.
5. Campos MK, Viana MB, de Oliveira BM, Ribeiro DD, Silva CM. Langerhans cell histiocytosis: A 16-year experience. J Pediatr (Rio J) 2007;83:79-86.
6. Howarth DM, Gilchrist GS, Mullan BP, Wiseman GA, Edmonson JH, Schomberg PJ. Langerhans cell histiocytosis: Diagnosis, natural history, management, and outcome. Cancer 1999;85:2278-90.
7. Guyot-Goubin A, Donadieu J, Barkaoui M, Bellec S, Thomas C, Clavel J. Descriptive epidemiology of childhood Langerhans cell histiocytosis in France, 2000-2004. Pediatr Blood Cancer 2008;51:71-5.
8. Puigdevall M, Bosio S, Hokama J, Maenza R. Langerhans cell histiocytosis of the atlas in the pediatric spine: Total reconstitution of the bone lesion after nonoperative treatment. A report of two cases. J Bone Joint Surg Am 2008;90:1994-7.
9. Jiang L, Liu ZJ, Liu XG, Zhong WQ, Ma QJ, Wei F, *et al*. Langerhans cell histiocytosis of the cervical spine: A single Chinese institution experience with thirty cases. Spine (Phila Pa 1976) 2010;35:E8-15.
10. McCarville MB. The child with bone pain: Malignancies and mimickers. Cancer Imaging 2009;9:S115-21.
11. Herman TE, Siegel MJ. Langerhans cell histiocytosis: Radiographic images in pediatrics. Clin Pediatr (Phila) 2009;48:228-31.
12. Khung S, Budzik JF, Amzallag-Bellenger E, Lambilliote A, Soto Ares G, Cotten A, *et al*. Skeletal involvement in Langerhans cell histiocytosis. Insights Imaging 2013;4:569-79.
13. Singh H, Kaur S, Yuvarajan P, Jain N, Maini L. Unifocal granuloma of femur due to Langerhans' cell histiocytosis: A case report and review of the literature. Case Rep Med 2010;2010. pii: 686031.
14. Azouz EM, Saigal G, Rodriguez MM, Podda A. Langerhans' cell histiocytosis: Pathology, imaging and treatment of skeletal involvement. Pediatr Radiol 2005;35:103-15.
15. Kumar N, Sayed S, Vinayak S. Diagnosis of Langerhans cell histiocytosis on fine needle aspiration cytology: A case report and review of the cytology literature. Patholog Res Int 2011;2011:439518.
16. Kilborn TN, Teh J, Goodman TR. Paediatric manifestations of Langerhans cell histiocytosis: A review of the clinical and radiological findings. Clin Radiol 2003;58:269-78.
17. Guobin H, Lingjing G, Xianglian D, Liqing S, Hong P, Qilan X. Clinical, pathological, and imaging characteristics of primitive neuroectodermal tumors of the spine. Diagn Interv Radiol 2014;20:168-71.
18. Momjian R, George M. Atypical imaging features of tuberculous spondylitis: Case report with literature review. J Radiol Case Rep 2014;8:1-14.